Mechanisms and consequences of horizontal gene transfer in cell wall-deficient cells of Kitasatospora viridifaciens

Kapteijn, R.

Chapter 5.

Vesicle formation by filamentous actinobacteria isolated from wastewater

Renée Kapteijn, Adelė Kaltenytė, David Calderón-Franco, Mark C. M. van Loosdrecht, Gilles P. van Wezel and Dennis Claessen

Abstract

Antimicrobial resistance is a major problem for public health, with an increasing number of infections by multidrug-resistant bacteria occurring worldwide. A major factor contributing to the spread of antibiotic resistance is horizontal gene transfer (HGT). Wastewater treatment plants (WWTPs) are considered a hotspot for the dissemination of antibiotic resistance due to the introduction of resistance genes and antibiotics to the high diversity of microbes present in this environment. Pathogens may acquire resistance from antibiotic producing soil bacteria such as *Streptomyces*, which contain multiple resistance genes per strain and are able to produce cell wall-deficient cells that can participate in HGT under laboratory conditions. In this study, 62 filamentous actinobacteria were isolated from a WWTP in The Netherlands, of which the majority was classified as *Streptomyces*. A quarter of the isolates, including *Streptomyces* and *Micromonospora* strains, produced large nucleic acid-containing vesicles upon exposure to hyperosmotic stress. These vesicles resemble cell wall-deficient cells that can potentially play a role in HGT in biofilm-like environments, such as activated sludge flocs in wastewater.

Introduction

Antimicrobial resistance (AMR) is a major threat to worldwide public health. AMR is the ability of microorganisms to survive exposure to drugs that would normally kill them or inhibit their growth [331]. An alarming report states that by 2050, ten million lives will be at risk annually due to drug resistant infections [26]. A major aspect of AMR is the resistance of bacteria to antibiotics, which is actually not a novel phenomenon. Antibiotics have existed since the early days of microbial life [332, 333], and may have provided their microbial producers an advantage in competition for resources, and antibiotic resistance genes (ARGs) have been detected in ancient permafrost samples [24] and isolated cave microbiomes [25]. However, the selective pressure brought about by the excessive anthropogenic use of antibiotics in medicine, aquaculture and agriculture has dramatically increased the evolution and spread of resistance, which now outpaces the development of new antibiotics [163, 334].

Bacterial antibiotic resistance can result from genetic changes such as mutations and the acquisition of new genetic information by horizontal gene transfer (HGT). These changes can lead to, for example, increased drug efflux, modification of the cellular target site or inactivation of the antibiotics themselves [335]. HGT is the transfer of genetic material between bacteria other than via reproduction, and can be promoted by low concentrations of antibiotics, non-antibiotic pharmaceuticals and other compounds [336-338]. HGT is considered a major driver for the spread of antibiotic resistance (ABR) [163, 337].

Wastewater and wastewater treatment plants (WWTP) are generally considered a hotspot for the dissemination of AMR [163, 174, 175]. In WWTPs, contaminated wastewater from households, hospitals, industrial and agricultural sites is collected and converted into cleaned water that can be discharged into the environment. Large solids are first removed by physical means during primary treatment, after which water is further purified by biological processes during secondary treatment [173, 334, 339]. WWTPs harbor a diverse microbial community that functions to degrade organic waste and remove carbon, nitrogen and phosphorous from the water during biological treatment [340, 341]. Bacteria are mainly present as microbial aggregates such as in surface-growing biofilm, granules or activated sludge flocs [334, 342]. The high microbial density and diversity in activated sludge, together with the presence of chemical and biological pollutants such as antibiotics, resistant bacteria and DNA carrying ARGs in wastewater may provide an environment conducive for the development and spread of AMR [163, 174, 175, 334, 343, 344].

It has been hypothesized that pathogenic bacteria can acquire resistance genes from soil-dwelling antibiotic producers [345, 346]. Nearly two-thirds of all known antibiotics originate from actinobacteria, of which the majority is produced by *Streptomyces* [6]. These filamentous bacteria produce antibiotics as part of their complex morphological differentiation. After formation of a substrate mycelium, part of this structure undergoes programmed cell death

(PCD) to release nutrients for the development of spore-bearing aerial hyphae [23, 24]. During PCD, antibiotics are produced to fend off other microbes that could utilize the released nutrients [13, 14]. Genes encoding proteins involved in the regulation and biosynthesis of secondary metabolites such as antibiotics, as well as genes related to resistance are typically localized in biosynthetic gene clusters (BGCs) [7, 30, 347]. An analysis of thirty *Streptomyces* genomes revealed the occurrence of around 20 to 45 BGCs per strain [31].

The discovery of similarity in enzymatic mechanisms employed by *Streptomyces* and pathogens to confer resistance to several antibiotics led to the 'producer hypothesis', suggesting that the enzymes may have originated from soil-dwelling actinobacteria [348-350]. This is supported by a study by Jiang *et al*., (2017) that identified proteins in proteobacteria with similarity to *Streptomyces* resistance proteins, including resistance to chloramphenicol and lincomycin [351]. *Streptomyces* has been isolated previously from WWTPs [352, 353] and can be detected in wastewater sludge samples by metagenomics and metatranscriptomics [354, 355]. In addition, metatranscriptomics analysis indicated the expression of genes involved in biosynthesis of streptomycin [354], an antibiotic produced by *Streptomyces griseus* [356], suggesting that *Streptomyces* can be actively present in wastewater environments.

Previous work (Chapter 3, Chapter 4) has shown that cell wall-deficient cells produced by *Kitasatospora viridifaciens*, closely related to *Streptomyces*, can participate in HGT. Upon growth under hyperosmotic stress conditions, *K. viridifaciens* produces temporary wall-deficient cells, called S-cells (from stress-induced cells), from the tip of the hyphae [15]. Prolonged incubation under hyperosmotic stress conditions results in the formation of permanently cell wall-deficient L-forms, which are named after the Lister Institute where this cell type was first described in 1935 [80]. S-cells and L-forms can be easily transformed with DNA using polyethylene glycol (PEG) and exchange DNA during co-culture (Chapter 3). In addition, L-forms can engulf plasmid DNA from their environment, leading to their transformation (Chapter 4). The switch to a wall-deficient lifestyle has been shown for *Streptomyces* and *Kitasatospora* strains isolated from Chinese mountain soil [15, 357], as well as for pathogenic bacteria such as *Listeria monocytogenes* [17], *Mycobacterium* sp. [270] and *Staphylococcus aureus* [271]. The switch to a wall-deficient state can be induced by hyperosmotic stress [15], inhibitors of cell wall synthesis such as antibiotics (as reviewed by Allan *et al*., 2009 [18]), or by exposure to bacteriophages [19, 20]. Wall-less bacteria require an osmotically stable environment to avoid bursting via osmotically-driven water uptake. Interestingly, the exopolysaccharide (EPS) component of biofilms functions as an osmolyte to increase the biofilm osmotic pressure [358-360], and cell wall-deficient bacteria have been detected in biofilms [111, 267, 268]. The combination of a dense microbial population in biofilms and activated sludge flocs, and the presence of antibiotics and bacteriophages may provide an environment that allows formation of wall-deficient cells in WWTPs.

Therefore, the aim of this study was to investigate the occurrence of bacteria capable of forming wall-less cells in a WWTP utilizing activated sludge, with a focus on filamentous actinobacteria. This research contributes to understanding the role of antibiotic-producing filamentous actinobacteria, as well as cell wall-deficient cells, in HGT in wastewater.

Results

Isolation of filamentous actinobacteria from wastewater

It is unknown whether filamentous actinobacteria capable of forming cell wall-deficient cells are present in wastewater systems. To study the presence of these bacteria in wastewater, samples were collected from the urban wastewater treatment plant (WWTP) Harnaschpolder (The Netherlands), which was followed by a selective isolation procedure (Fig. 1A). Two samples were obtained from the first stage of wastewater treatment, namely before and after primary sedimentation (BPS and APS, respectively) (Fig. 1B). Another sample was obtained after the second treatment stage, the biological treatment stage, containing activated sludge (AS). Activated sludge was an especially turbid suspension that contained large clumps and small organisms such as ciliates (Fig. 1B, C). To isolate filamentous actinobacteria, dilutions were placed on five different isolation media, namely Humic acid Vitamin agar, Czapek Dox agar, Starch Casein agar, MS medium and Minimal Medium agar, which were incubated at 30 °C. One sample of AS was treated with the detergent Nonidet to break up the sludge flocs (AS-N) [361]. Each week, isolation plates were inspected for new colonies, which were marked and subsequently streaked on the same isolation medium as well as on ISP-2 medium [362, 363], both containing nalidixic acid and nystatin to inhibit growth of Gram-negative bacteria and fungi, respectively [357] (Fig. 1D). Upon confirmation of filamentous growth and the absence of contamination by microscopy, isolates were grown confluently on MS medium to obtain spores, or were grown in liquid TSBS medium when sporulation was not observed on solid medium. Spores and/or mycelial biomass was stored in glycerol at – 80 °C until further use.

A total of 62 putative actinobacteria were isolated, each designated a unique number preceding 'HP' (from 'Harnaschpolder' WWTP). The isolation medium yielding most strains was MS medium (19 isolates) followed by Starch Casein (SC, 15 isolates)(Fig. 1E), while most isolates originated from the AS samples (Fig. 1F). The majority of isolates had a typical *Streptomyces* morphology with a non-shiny, wrinkly, and 'fluffy' appearance indicating aerial hyphae, and the biomass was often growing into the agar. Longer incubation typically resulted in droplets appearing on the surface of the colonies, suggesting the production of secondary metabolites (Fig. 1G – HP37). Three isolates did not appear to form aerial hyphae (HP7, HP52 and HP58) and formed biomass that was orange in colour (Fig. 1G – HP7) (Supplementary Fig. 1A).

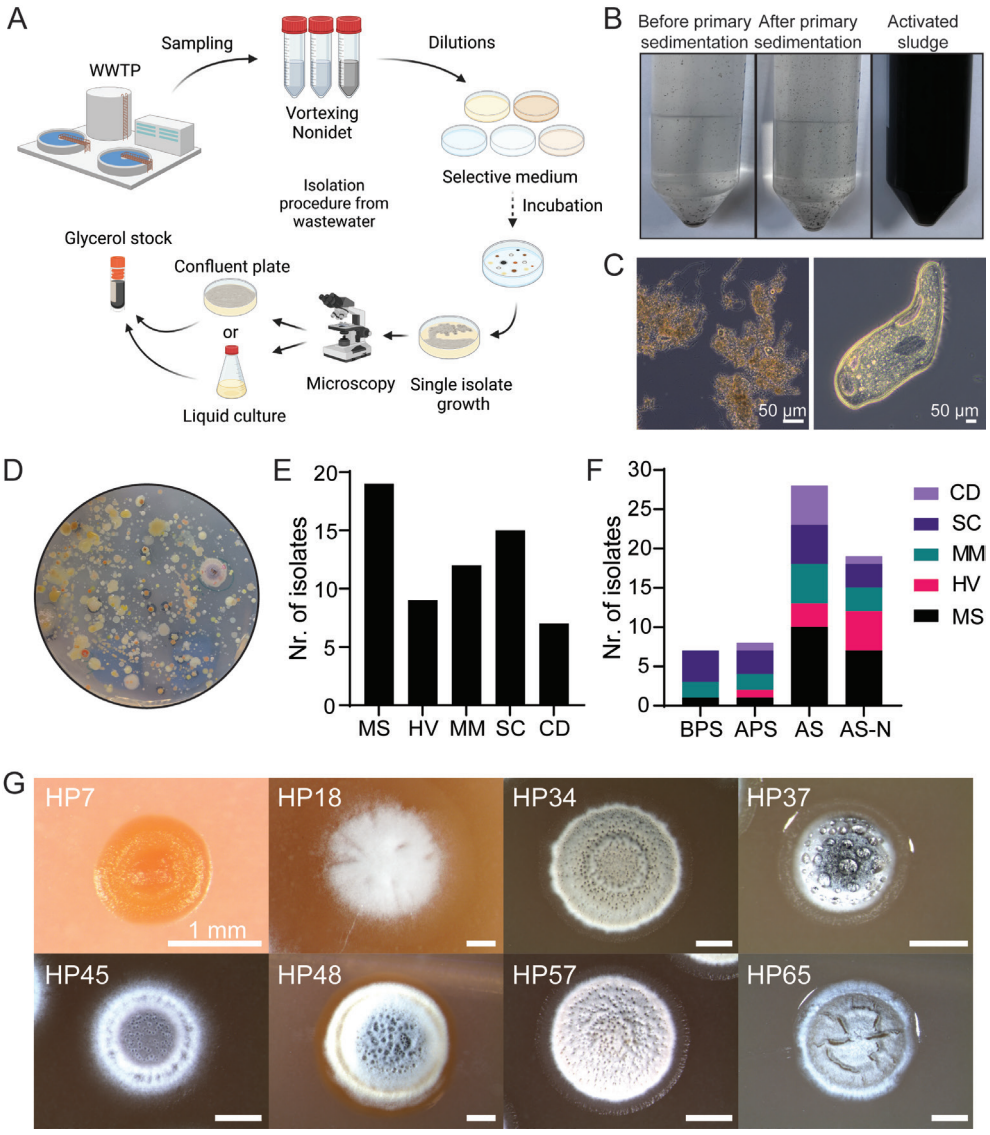

Figure 1. Isolation of filamentous actinobacteria from wastewater

(A) Schematic representation of the isolation of filamentous actinobacteria from the Harnaschpolder wastewater treatment plant (WWTP), The Netherlands. Three wastewater samples (before and after primary sedimentation and activated sludge) were obtained. Samples were resuspended by vortexing, and activated sludge was treated with and without the detergent Nonidet. Subsequently, dilutions were plated on selective isolation medium. Isolation medium was inspected for the formation of colonies for up to four weeks, after which *Streptomyces*-like colonies were streaked on solid medium to obtain pure isolates. After confirmation of filamentous growth and absence of contamination by microscopy, isolates were confluently grown on MS medium or in liquid TSBS medium (in case no aerial hyphae with spores developed). Cells were resuspended in glycerol for long term storage at – 80 °C. **(B)** Wastewater samples, note the turbid activated sludge sample which contained many clumps (see also panel **C**). **(C)** Micrographs of the activated sludge sample. Note the aggregates (left) and the presence of ciliates (right). **(D)** Example of isolation plate (Minimal Medium) after three weeks of incubation. Despite the use of selective medium, many differently shaped colonies were observed. **(E)** Number of isolates obtained from the different isolation medium plates. MS: Mannitol

Soya Flour medium, HV: Humic acid Vitamin agar, MM: Minimal medium, SC: Starch Casein agar, CD: Czapek-Dox agar. **(F)** Number of isolates obtained from the different wastewater samples. BPS: Before primary sedimentation sample, APS: After primary sedimentation sample, AS: Activated sludge sample, AS-N: Activated sludge sample treated with Nonidet. **(G)** Stereomicroscope images showing single isolate colonies after growth on MS medium for up to 168 h. Note that the majority of colonies had a dry, fuzzy surface representing aerial hyphae, as well as hyphae with a darker colour that may indicate spore formation. Droplets on top of the biomass (HP37) may indicate the production of secondary metabolites. HP7, HP58 and HP52 had a shiny, orange biomass without aerial hyphae (Supplementary Fig. 1A).

Phylogenetic characterization of wastewater isolates

To confirm the isolation of filamentous actinobacteria, the 16S rRNA gene from each isolate was amplified by PCR and was partially sequenced with a minimum of 1 kb sequence data (Supplementary Table 1). A comparison of the partial 16S rDNA sequences of the isolates to the known strains from the EzBioCloud database [364] indicated that 58 out of 62 strains had a high similarity (in the range of 97.6% – 100% pairwise identity) to strains belonging to the genus *Streptomyces* (Supplementary Table 1).

Interestingly, the three isolates that did not produce aerial hyphae (HP7, HP52 and HP58) had more than 99% similarity to strains belonging to the genus *Micromonospora* (specifically, *M. aurantiaca, M. fluminis* and *M. vinacea*, respectively). Indeed, the orange biomass colour of the *Micromonospora*-like isolates is typical of *Micromonospora* [365] (Supplementary Fig. 1A). In addition, the 16S rDNA gene sequence of HP47 was most similar to that of *Pseudonocardia carboxydivorans*. In agreement, the brown substrate mycelium and white aerial mycelium of HP47 is similar to this characterized species [366] (Supplementary Fig. 1B).

Based on the 16S rDNA data, multiple isolates had the highest similarity to the same database strain, such as for the isolates HP14, 20, 26, 42, 43, 64 and 65 which were all most similar to *S. albidoflavus* DSM 40455 (Supplementary Table 1). As the same wastewater samples were placed on five different isolation media, it is possible that the same strain was isolated multiple times. To gain insights into the diversity of the isolates, a phylogenetic tree was constructed based on partial 16S rDNA sequences. To compare the isolates to a set of diverse species, 27 *Streptomyces* species and one *Kitasatospora* species (hereafter all referred to as streptomycetes) from different branches of an extensive phylogenetic tree containing 1020 *Streptomyces* and *Kitasatospora* strains [367] were included, in addition to *S. coelicolor*, *S. griseus* subsp. *griseus* and *S. clavuligerus*. After multiple sequence alignment, the 16S rDNA sequences were trimmed to 897 bp (with gaps), corresponding to nucleotide positions 141 – 1037 of the *S. coelicolor* 16S rRNA gene (*rrnB*) [368], and were used to generate a phylogenetic tree. *Nitriliruptor alkaliphilus* was used as an outgroup as it belongs to the Nitriliruptoria, the class most closely related to Actinobacteria [369, 370 371].

The resulting phylogenetic tree separated the *Micromonospora* (HP7, HP52, HP58) and *Pseudonocardia* (HP47) isolates from the *Streptomyces* isolates (Fig. 2). Additionally, two

large clades were present within the *Streptomyces* clade: one containing *S. coelicolor* and one containing *S. griseus* subsp. *griseus*. However, the bootstrap confidence values for these two clades as well as several other clades were low (under 60%) [33, 372]. The tree also contained polytomies (internal nodes with more than two descendants), which likely indicate a lack of sufficient data from the partial 16S rDNA sequences to resolve the evolutionary relationships [373]. Indeed, the genus *Streptomyces* has been challenging to taxonomically characterize by 16S rDNA due to limited variation in this gene, thereby not resulting in sufficient resolution [33, 374]. The protein sequence of the conserved sporulation protein SsgA has been previously used to study the morphological characteristics and evolutionary divergence of *Streptomyces* sp. [374]. Specific amino acid residues at key positions in the SsgA protein sequence correlate with the submerged sporulation ability of Streptomycetes [374], namely non-liquid sporulation (NLSp) and liquid sporulation (LSp) phenotypes. Therefore, the *ssgA* nucleotide sequence was amplified and sequenced (near-complete) for all *Streptomyces* isolates (note that the *Micromonospora* and *Pseudonocardia* isolates were not included due to the lack of *ssgA*). The *ssgA* sequences from the isolates and the 31 known streptomycete strains were aligned, trimmed (394 bp with gaps, corresponding with nt position 6 – 399 of *S. coelicolor ssgA*) and translated to protein sequences. This was followed by a multiple sequence alignment (MSA) of the SsgA protein sequences (pos. 2-133 corresponding to *S. coelicolor* SsgA)(Supplementary Fig. 2). Based on the presence of the key amino acid residues in the SsgA protein sequence [374], 16 isolates were assigned as putative NLSp strains and 20 isolates as putative LSp strains. For some strains the SsgA contained residues belonging to both types of liquid-sporulation phenotypes (Supplementary Fig. 2).

Two phylogenetic trees were generated based on the near-complete SsgA nucleotide (Fig. 3, Supplementary Fig. 3) or protein sequences (Supplementary Fig. 4). Both trees largely separated the strains by their predicted ability to produce submerged spores (LSp: magenta text, NLSp: green text) as was also indicated by the clustering with *S. coelicolor* (NLSp)[375] or *S. griseus* subsp. *griseus* (LSp) [376]. In addition, the phylogenetic tree grouped 11 strains (consisting of HP62, HP63 and the clade containing *S.* sp. NRRL B-3253, indicated in blue text). Based on the MSA of SsgA protein sequences, the amino acid residues at the key positions of SsgA from these 11 strains fully matched with the residues of SsgA from *S. albus* (Supplementary Fig. 2). *S. albus* does not sporulate in liquid-grown cultures, but forms open mycelial structures rather than the large clumps typical of NLSp strains [374]. In addition, *S. albus* SsgA differs in four of the six key residues typically found in NLSp strains [374]. These 11 strains might therefore represent a subgroup within the NLSp phenotype.

Comparing the 16S rDNA and *ssgA* nucleotide sequences between isolates revealed that seven pairs contained identical partial sequences and are likely closely related, if not the same strain (Supplementary Table 2, top rows). In addition, ten pairs contained identical 16S rDNA but different *ssgA* sequences, and eight pairs contained identical *ssgA* sequences but

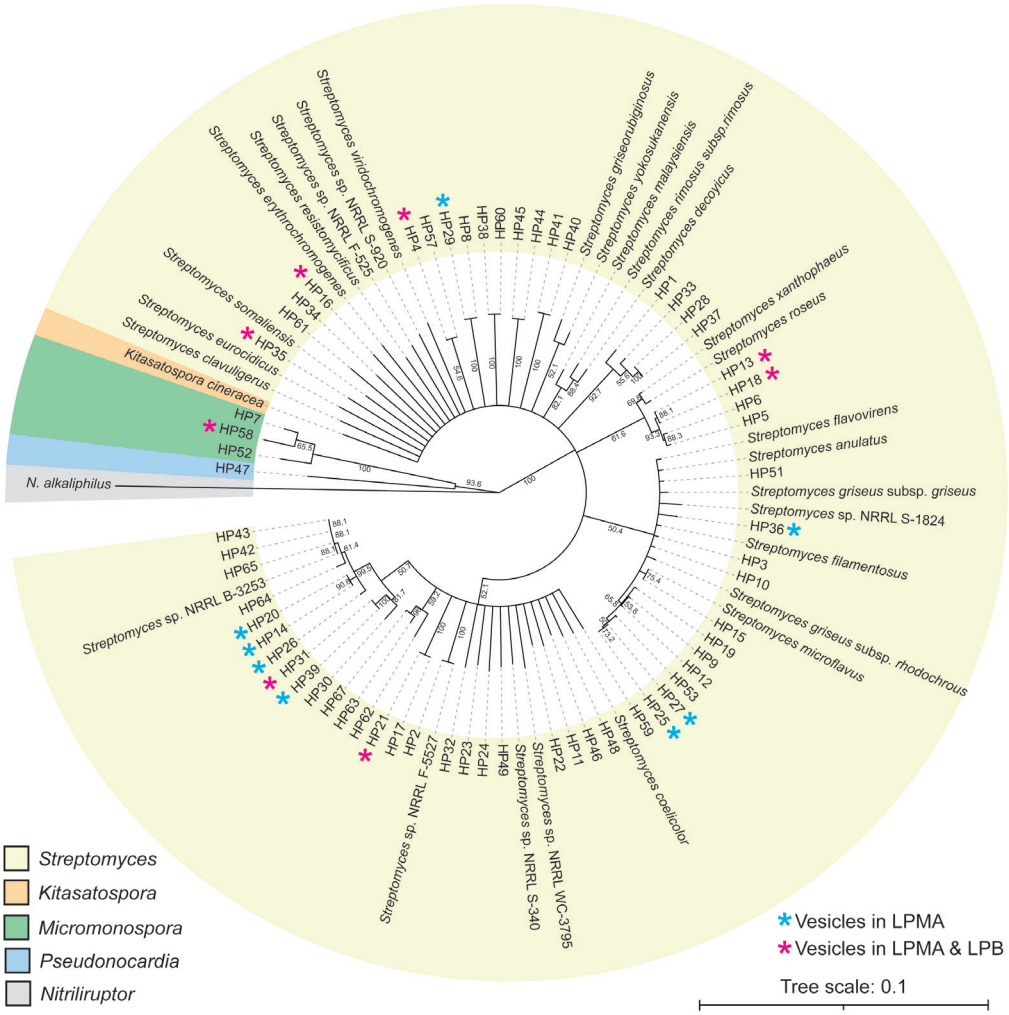

Figure 2. Phylogenetic tree based on partial 16S rDNA sequences

Neighbor-joining phylogenetic tree based on partial 16S rDNA sequences (897 bp with gaps) of 62 wastewater isolates (HP), 30 known *Streptomyces* strains and one *Kitasatospora* strain. *Nitriliruptor alkaliphilus* was used as an outgroup. The consensus tree was constructed based on the Neighbor-Joining algorithm with Tamura-Nei Genetic Distance model. The numbers at the nodes indicate bootstrap support values based on 1000 replicates. Different genera are indicated by background shading as following: yellow – *Streptomyces*, orange – *Kitasatospora*, green – *Micromonospora*, blue – *Pseudonocardia*, grey – *Nitriliruptor*. The scale bar represents 0.1 nucleotide substitutions per position. Asterisks (*) indicate the ability to form vesicles on solid LPMA and liquid LPB medium (magenta) or only on LPMA medium (blue), which was only tested for the HP isolates.

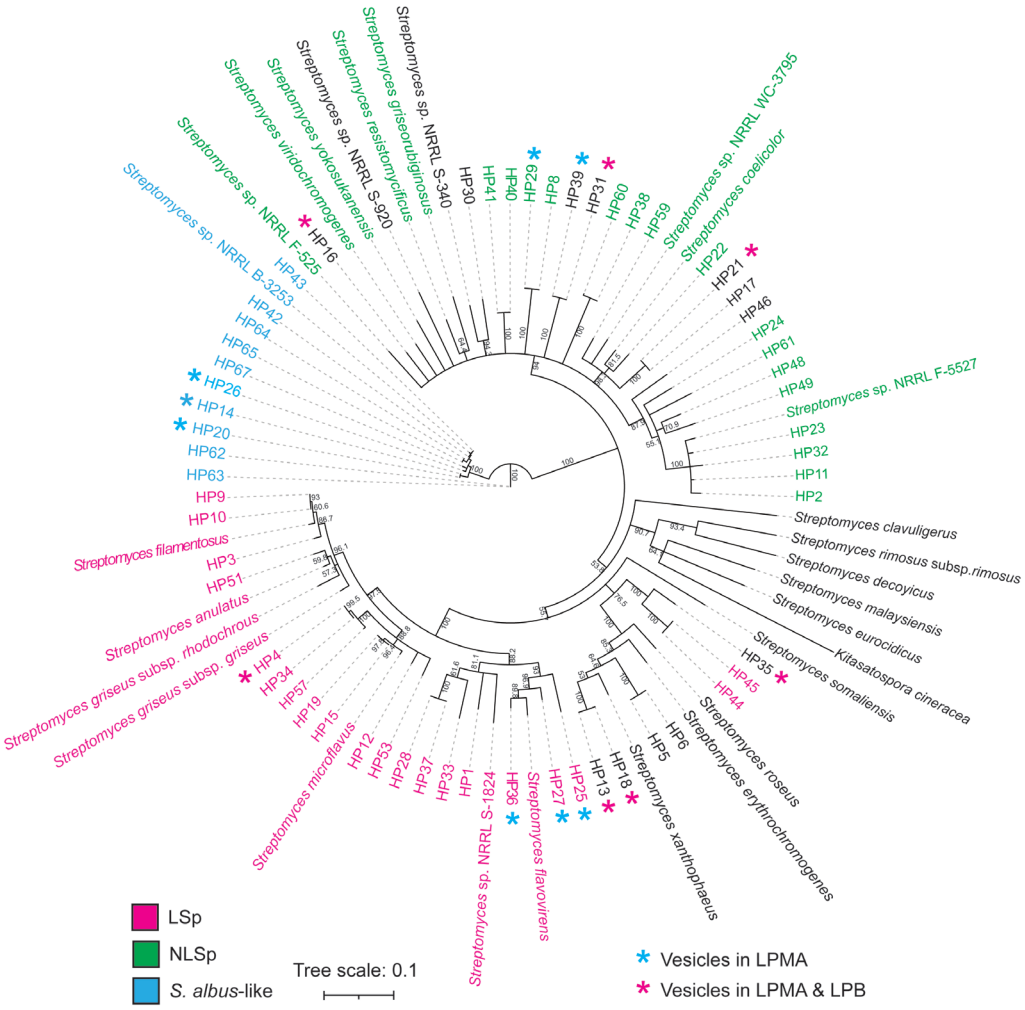

Figure 3. Phylogenetic tree based on *ssgA* nucleotide sequences

Neighbor-joining phylogenetic tree based on near-complete *ssgA* sequences (394 bp with gaps) of 58 wastewater isolates (HP), 30 known *Streptomyces* strains and one *Kitasatospora* strain. The consensus tree was constructed based on the Neighbor-Joining algorithm with Tamura-Nei Genetic Distance model. The numbers at the nodes indicate bootstrap support values based on 1000 replicates. The scale bar represents 0.1 nucleotide substitution per position. Asterisks (*) indicate the ability to produce vesicles on solid LPMA and liquid LPB medium (magenta) or only on solid LPMA medium (blue), which was only tested for the HP isolates. Coloured text indicates strains having all SsgA protein sequence key residues that are exclusively found in liquid-culture sporulation (LSp, magenta) or non-liquid sporulation (NLSp, green) phenotypes (See Supplementary Fig. 2). Blue colouring indicates strains with key residues that correspond to *S. albus* SsgA. Strains having only part of, or a mix of LSp and NLSp SsgA key residues are indicated with black text. See also Supplementary Fig. 3 for magnified section of the tree (*S-albus*-like).

differing 16S rDNA sequences. Therefore, even incomplete sequencing of multiple genes can be valuable to establish differences between isolated bacteria. All in all, the sequencing analysis revealed that a set of genetically and morphologically diverse actinobacteria, belonging to the genera *Streptomyces*, *Micromonospora* and *Pseudonocardia*, have been isolated, consisting of mostly unique isolates.

Formation of large vesicles under hyperosmotic stress conditions

To determine if the wastewater isolates can form cell wall-deficient cells upon exposure to hyperosmotic stress, the strains were grown on solid LPMA (L-phase medium agar) medium containing 20% (w/v) sucrose [15]. After 72 h incubation, vesicles resembling wall-less S-cells were detected by microscopy for 16 of the 62 isolates (Supplementary Table 3). This included vesicles with a diameter larger than 2 µm, as was previously used to differentiate small S-cells from spores [15]. In addition to the *Streptomyces* isolates, spherical cells were observed for the *Micromonospora* isolate HP58. Prolonged incubation of HP58 in liquid TSBS medium resulted in structures seemingly similar to the vesicles, but were attached to the hyphal tips. These structures could actually be single spores as produced by *Micromonospora* sp., but they also shared resemblance with S-cells that are extruded from the tip of the hyphae in *K. viridifaciens* [15]. To exclude that the spherical cells produced on LPMA medium are spores, biomass from HP58 grown in liquid TSBS medium or on solid LPMA medium was exposed to water or osmotically protective LPB medium. Whereas TSBS medium-induced spherical structures were still observed after treatment with water, spherical cells induced on LPMA medium were hardly detected, suggesting that they had burst due to the osmotic downshift (Supplementary Fig. 5). This strongly suggests that a high osmotic pressure induces the production of wall-less cells in *Micromonospora*.

Subsequent growth of the 16 vesicle-forming isolates in liquid LPB medium for 48 h resulted in the detection of vesicles for 8 out of 16 isolates. The presence of membrane and nucleic acids in these vesicles was confirmed for all strains by confocal microscopy after staining cell samples from LPMA or LPB medium with SynapseRed and SYTO 9, respectively. All isolates had the ability to produce nucleic-acid containing vesicles, likely containing DNA, larger than 2 µm in diameter. Vesicles seemingly devoid of nucleic acids were sometimes also detected, as shown for HP58 and HP39 (Fig. 4A - HP58 white arrow, Fig. 4B - HP39). Putative empty vesicles were also observed for HP13 (cultured in LPB medium) as suggested by a very light colour (Fig. 4B). These results suggest that the large vesicles produced by the wastewater isolates indeed resemble S-cells induced by hyperosmotic stress, however, not all extruded vesicles contain chromosomal DNA.

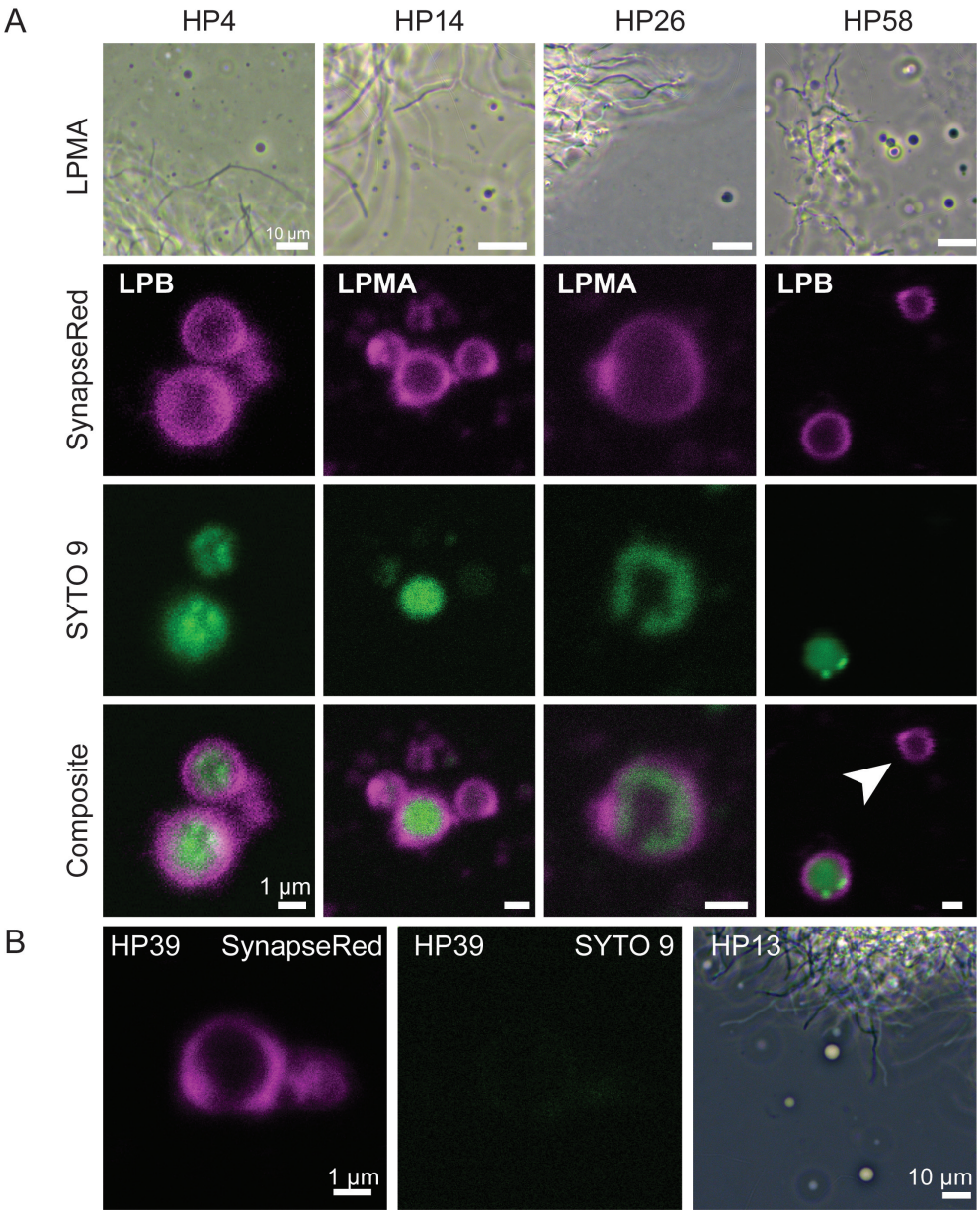

Figure 4. Vesicle formation by wastewater isolates

(A) Micrographs indicating the formation of vesicles resembling wall-deficient cells by isolates HP4, 14, 26 and 58. Light microscopy (top row) was performed after growth for 72 h on LPMA medium (96 h for HP58) followed by resuspension in LPB medium for microscopy. Note the differently sized vesicles. Fluorescence micrographs were obtained after 72 h of growth in LPB medium or on LPMA medium as indicated. Cell membranes were visualized with SynapseRed (magenta) and nucleic acids with SYTO 9 (green). Arrow indicates a vesicle lacking nucleic acids. Scale bars represent 1 µm. **(B)** Fluorescence micrographs of HP39 and light microscopy of HP13 grown for 72 h in LPB medium showing putative empty vesicles due to a lack of SYTO 9 staining (HP39) or light colour (HP13).

The ability to form large vesicles was not restricted to certain clades on the 16S rDNA or SsgA-based phylogenetic trees (both SsgA nucleotide and protein sequence-based trees) (vesicle-forming isolates indicated by asterisks in Fig 2, 3 and Supplementary Fig. 3, 4). Isolates HP13 and HP18 had a similar morphology on MS medium (Supplementary Fig. 6), identical partial 16S rDNA and *ssgA* nucleotide sequences and both formed vesicles on LPMA and LPB medium (Supplementary Table 2). However, isolates HP17 and HP21 had identical or near-identical 16S rDNA and *ssgA* sequences, a similar phenotype on MS medium (Supplementary Fig. 6), but vesicles were formed by HP21 and not HP17 (Supplementary Table 2). This suggests that closely related strains can respond differently to osmotic stress and similarity in partial 16S rDNA and *ssgA* sequences is not sufficient to predict their ability to form putative S-cells.

These results indicate that filamentous actinobacteria capable of forming large, nucleic acid-containing vesicles, most likely representing S-cells, can be present in wastewater treatment systems. The production of such vesicles is not limited to the known *Streptomyces* and *Kitasatospora* genera but includes the filamentous *Micromonospora* genus. The response to form large vesicles upon growth under osmotically stressful conditions is found among genetically and morphologically diverse species and can differ between closely related strains.

Discussion

HGT is a major driver for the dissemination of antibiotic resistance genes in the environment [163, 337, 377], and WWTPs are considered a hotspot for the spread of resistance [174, 378]. Previous work indicated that the switch to a wall-deficient lifestyle enables HGT in the filamentous actinobacterium *K. viridifaciens* (Chapter 3, 4). Wall-deficient cells have been detected in biofilms, which is a structure that can be present in activated sludge of WWTPs. This study confirmed the presence of filamentous actinobacteria in a Dutch urban WWTP. A quarter of actinobacterial isolates produced large nucleic-acid containing vesicles upon growth in hyperosmotic stress. This ability was not limited to the *Streptomyces* genera and included a strain belonging to *Micromonospora*. This research provides the basis to further elucidate the role of such structures in wastewater and HGT.

A total of 62 bacterial strains were isolated from wastewater, with the majority originating from activated sludge samples. WWTPs maintain a high diversity of microbes in the activated sludge tank that perform the biological treatment of wastewater [340]. Comparison of the nucleotide similarity of partial 16S rDNA with known bacterial species indicated all isolates were actinobacteria, of which 58 belonged to the genus *Streptomyces*, three to *Micromonospora* and one isolate belonged to the genus *Pseudonocardia*, which was in line with their phenotypic characteristics. Actinobacteria belonging to these genera have been previously isolated from WWTPs [352, 353, 379, 380], although *Pseudonocardia* is rarely found [353].

Streptomycetes are mainly of interest for wastewater treatment as a source of enzymes for the bioconversion of industrial waste products such as synthetic dyes, lignin, fats and oils [381, 382], as well as for the production of bioflocculants [383, 384]. In addition, *Streptomyces* bacteria are also used in biological treatment to remove organic matter [352, 385], for bioremediation of heavy metals [386] and in processes that use bacterial consortia to couple wastewater treatment to biodiesel production [387, 388].

Growth of the wastewater isolates under hyperosmotic stress conditions revealed that 16 out of 62 isolates were capable of producing vesicles containing nucleic acids, most likely indicating DNA, that resemble S-cells as described for *K. viridifaciens* [15]. This ability could not be explained by evolutionary relatedness based on partial 16S rDNA or their predicted submerged sporulation phenotype (SsgA), which is in line with findings from Ramijan *et al*., (2018) [15]. Some strains of *Micromonospora* produce small membrane vesicles, as observed using electron microscopy [389, 390]. To the best of our knowledge, this is the first report of the production of large vesicles resembling cell wall-deficient cells by *Micromonospora*. The ability to produce wall-less cells amongst filamentous actinobacteria is thus likely more widespread than previously thought. Despite high similarity in 16S rDNA and *ssgA* sequences, the isolates had different vesicle formation abilities in response to sucrose as osmolyte. More elaborate tests using different osmolytes and longer incubation times may extend the number of isolates forming vesicles.

The ability of *Micromonospora*, *Kitasatospora* and *Streptomyces* to produce wall-less cells may be linked to their polar mode-of-growth. In filamentous actinobacteria, new cell wall material is incorporated at the tip of the hyphae [253, 391], resulting in extensive cell wall remodeling that may enable the extrusion of wall-less cells or extracellular vesicles [59, 181]. Extrusion of wall-less cells has indeed also been observed in polar-growing mycobacteria [270]. Recently, it was shown that the deletion of a gene encoding the stomatin-like protein StlP, a protein that localizes at hyphal tips and plays a role in coordinating tip growth, enables the formation of wall-deficient cells by *S. coelicolor* [118]. It would be interesting to analyze the presence of StlP across *Streptomyces* species, to test if there is a relationship between StlP and the ability to form cell wall-deficient cells. The extrusion of wall-less cells by mycelial bacteria most likely leads to the release of only part of the cytosol and cytoplasmic membrane, rather than resulting in a complete shift to wall deficiency. Phenotypic heterogeneity may be a way to adapt to changing environments in which it is beneficial to switch between walled and wall-less morphologies.

Wall-less bacteria can, at least temporarily, survive environments such as plant tissue [110, 114], urine [21], insect hemolymph [112], zebrafish tissue [21] and biofilms [111, 267, 268]. Actinobacteria such as *Micromonospora*, *Kitasatospora* and *Streptomyces* can live in close interaction with plants and have been isolated from rhizosphere soils, roots and plant nodules [8, 392]. The vesicle forming isolate HP58 was most closely related to *Micromonospora vinacea* GUI63 that was

isolated from root nodules of the pea plant *Pisum sativum* [393]. The production of wall-less cells may enable bacterial transportation via plant sap [114] which contains a high level of sugar, providing an osmotically protective environment.

The detection of wall-less cells in biofilms raises questions regarding their potential presence and role in environments such as wastewater. Bacteriophages are abundantly present in wastewater [394], as well as cell wall-targeting antibiotics such as amoxicillin and cefuroxime [395, 396]. Cell wall-targeting agents may induce the formation of wall-less cells, providing there is sufficient osmotic protection, such as in the EPS component of biofilms or sludge flocs. Alternatively, the disruption of cell wall-deficient cells due to contact with water will result in release of nucleic acids, which may contribute to EPS production and floc formation. Release of DNA may increase the availability of extracellular DNA (eDNA) encoding ARGs or DNA that harbors mobile genetic elements such as transposable elements or plasmids in wastewater [344], thereby promoting HGT.

The sequencing of *ssgA* resulted in the putative classification of the majority of wastewater isolates in either NLSp or LSp groups, based on key residues in the SsgA protein sequence [374]. Eleven strains contained key SsgA residues that correspond to the atypical *S. albus* SsgA sequence. Further study of the morphology of strains with an *S.albus*-like SsgA protein sequence could lead to the recognition of a sub-class within the NLSp group, enabling improved morphological classification of *Streptomyces* strains. In addition, the extensive analysis of SsgA sequences indicated that several strains had part of the key residues in the SsgA protein sequence corresponding to an NLSp phenotype, while other key residues corresponded to the LSp phenotype. Although this made it difficult to predict the submerged sporulation phenotype based on SsgA alone, this diversity may reflect the evolution of SsgA. These results indicate that there likely is more subtle diversity in *Streptomyces* submerged sporulation phenotypes in addition to the established NLSp and LSp groups.

Although many filamentous actinobacteria were isolated from wastewater, around a quarter of which was capable of formation of vesicles resembling wall-deficient S-cells, this data does not necessarily indicate that the isolates were actively growing in the wastewater, let alone producing wall-less cells. The isolates could have merely resided in the wastewater as dormant spores. Additional studies to examine the presence of wall-less cells in wastewater should be conducted. This can include the resuspension of biofilm or flocs in an osmotically protective and unprotective solution followed by the assessment of cell morphology by flow cytometry and microscopy, possibly using fluorescence in situ hybridization (FISH) [397, 398]. This can be combined with isolation procedures for wall-less bacteria that are based on their intrinsic properties, such as their ability to pass through 0.45 µm filters or resistance to cell wall-targeting compounds [21, 399].

Summarizing, in this study a large diversity of filamentous actinobacteria was isolated from a WWTP in The Netherlands. Growth of these isolates under hyperosmotic conditions

induced the formation of nucleic acid-containing vesicles, resembling wall-deficient cells, in a quarter of the isolates. Although it is not known whether such vesicles are produced in WWTPs, the EPS component of activated sludge flocs and biofilms may form a sufficiently protective environment. Wall-less cells may play a role in HGT by the release of DNA after cell disruption, via vesicle-mediated DNA exchange or uptake of extracellular DNA. Further research is required to elucidate the role of wall-deficient cells in HGT or EPS formation in wastewater.

Materials and methods

Sample collection and selective isolation of filamentous actinobacteria

Wastewater samples were obtained from the wastewater treatment plant (WWTP) Harnaschpolder (Waterboard Delfland, The Netherlands) on 28th September 2020 and kept at 4 °C for 24 h until use. Samples were briefly vortexed before dilutions were prepared in sterile tap water. 100 µl samples were placed on five different media containing 10 µg ml^{-1} nalidixic acid and 50 µg ml^{-1} nystatin to repress the growth of Gram-negative bacteria as well as fungi [357]. The following isolation media were used: Mannitol soya flour medium (MS), Humic acid Vitamin agar (HV), Czapek-Dox agar (CD), Starch casein agar (SC) and Minimal medium supplemented with 1% (v/v) glycerol (MM) (Supplementary Table 4). Plates were inspected for the formation of mycelial colonies every seven days during four weeks. Colonies were selected based on a wrinkly, dry, non-shiny or leather-like appearance, as well as presence of spore-bearing aerial hyphae. Morphological analysis was aided by a Leica M80 Stereo Zoom microscope with a Leica KL1500 LCD Fiber Optic Light Source, connected to a Bresser MikroCam SP 5.0 and Bresser MikroCamLab II software version ×64, which was also used to image single colonies. Potential filamentous actinobacterial colonies were streaked on the same medium used for the isolation, while also streaking them on International Streptomyces Project medium 2: yeast extract - malt extract agar (ISP-2, containing 4 g yeast extract, 10 g malt extract and 4 g dextrose per liter) [362, 363], both containing nalidixic acid and nystatin. Biomass was examined for mycelial growth and potential contamination after incubation at 30 °C using a Zeiss Axioscope A.1 linked to a Axiocam 105 color camera (Zeiss), using the ZEN 2.5 software (blue edition, Carl Zeiss Microscopy GmbH). When contamination was present, multiple single colonies were streaked on MS medium containing nalidixic acid and nystatin. For long-term storage, isolates were grown confluently on MS medium or maltose-yeast extract medium (MYM) [222], after which spores or the biomass was harvested with a cotton swab and stored in 20% glycerol at – 80 °C. Isolates that did not produce aerial hyphae were grown in TSBS medium until sufficient growth was obtained, and were resuspend and stored in 20% glycerol at – 80 °C. Final assessment of the absence of contamination of

the stocks was performed by growth in LB medium and Tryptone Soya Broth medium [223] containing 10% (w/v) sucrose (TSBS medium).

Primer design and PCR amplification of 16S rDNA and *ssgA*

The universal degenerate primers F27 (5' AGAGTTTGATCMTGGCTCAG 3') and R1492 (5' TACGGYTACCTTGTTACGACTT 3') [400] (spanning positions 7 to 1497 of 16S rDNA *rrnB* in *S. coelicolor*) were used to amplify a ~ 1.5 kbp product to obtain the 16S rRNA gene sequence. For amplification of *ssgA*, predicted *ssgA* sequences with 500 bp flanks were obtained from the StrepDB database (http://strepdb.streptomyces.org.uk/, accessed Nov. 2022)(Supplementary Table 5). Multiple sequence alignment was performed using Clustal Omega v. 1.2.2 [401] with standard settings in Geneious Prime v. 2022.1.1. Degenerate primers for *ssgA* amplifications were designed based on the most conserved regions in the *ssgA* flanking sequences [402], resulting in ssgA_FW_deg (5' CAGYATCTGAAAAMTCACTCCTTG 3') and ssgA_RV_deg (5' CTBTTCTCSATCGCSCAGAGC 3'), which amplifies a ~ 800 – 1100 bp region. To prepare template for PCR amplifications, isolates were first inoculated from the frozen stock in TSBS medium in a coiled flask and grown at 200 rpm and 30 °C for up to 72 h. Around 1 – 2 ml of the culture was pelleted by centrifugation at 2000 ×*g* for 10 min, after which the pellet was washed with MilliQ and frozen at – 20 °C until use. A swab (~ 4 µl) of biomass was resuspended in 50 µl MilliQ and boiled for 10 min to lyse cells. Around 2 µl of lysed cells was used as DNA template per 50 µl PCR (Polymerase Chain Reaction) volume. In case no PCR product was obtained, gDNA was isolated (as described in Kieser *et al*., 2000 [223]) and 1 µl of diluted gDNA was used as a template.

Sanger sequencing was performed at Macrogen Europe, Amsterdam using ssgA_FW_seq (5' ATCTGAAAAMTCACTCCTTG 3') or Seq F1 [357] (5' TGCTTAACACATGCAAGTCG 3') for *ssgA* and 16S rDNA, respectively. Ambiguous bases were resolved using reverse primers R1492 and ssgA_RV_deg for 16S rDNA or *ssgA*, respectively.

Phylogenetic analysis

Sanger sequences were quality trimmed using the 'Trim Ends' option under 'Annotate & Predict' using standard settings in Geneious Prime v. 2022.1.1. In cases that a single sanger sequencing run did not provide a sufficiently long product, a consensus sequence using multiple sanger sequences was generated using the 'De Novo Assembly' option with the assembler method 'Geneious' on 'Highest Sensitivity/Slow'. The trimmed 16S rDNA sequences were used to compare against 16s rDNA sequences present in the EzBioCloud database [364].

25 representatives were selected from a phylogenetic tree of *Streptomyces* and *Kitasatospora* species [367], along with *Streptomyces coelicolor* A3(2), *Streptomyces griseus* subsp. *griseus* and *Streptomyces clavuligerus* (Supplementary Table 6). Genome assemblies of these strains were obtained from NCBI. The 16S rDNA and putative *ssgA* sequences were

extracted based on annotations or based on highest similarity with *rrnB* or *ssgA* (SCO3926) of *S. coelicolor* A3(2), respectively, using offline BlastN in Geneious Prime. In the cases that multiple intact, but slightly different 16S rRNA genes were available for the representative species, the sequences were aligned using Clustal Omega v. 1.2.2 in Geneious Prime and a consensus sequence was generated with 100% identity to include all nucleotide varieties.

Multiple sequence alignment of the 16s rDNA and *ssgA* nucleotide sequences was performed using Clustal Omega v. 1.2.2. A 897 bp-region (including gaps, corresponding with nt position 141 to 1037 of *S. coelicolor rrnB*) and a ~ 394 bp-region of *ssgA* (corresponding with nt position 6 – 399 of *S. coelicolor ssgA*) was extracted for all isolates and representative species. Extracted *ssgA* nucleotide sequences were translated (relative to pos 7 – 399 of *ssgA* of *S. coelicolor* A3(2) or amino acid position 3 - 133) to obtain the protein sequence. Multiple sequence alignment of SsgA was visualized using Jalview v. 2.11.2.0 [403].

Phylogenetic trees were constructed based on the Neighbor-Joining method [404]with the Tamura-Nei Genetic Distance model [405] as previously described by Labeda *et al*., (2012) [33] using the 'Geneious Tree Builder'. A consensus tree was created using 1000 bootstrap replicates [372], and nodes with bootstrap support values lower than 50 were collapsed. The 16S rRNA gene (NITAL_RS17080) of the actinobacterium *Nitriliruptor alkaliphilus* DSM 45188 belonging to the class 'Nitriliruptoria' [369] was used as an outgroup for the 16S rRNA gene tree. Phylogenetic trees were visualized using iTol [406].

Detection of vesicle formation

Spores or mycelial biomass was plated on LPMA (L-phase medium agar, containing 20% (w/v) sucrose, 0.5% (w/v) glucose, 0.5% (w/v) yeast extract, 0.5% (w/v) peptone, 0.01% (w/v) $MgSO_4 \times 7H_2O$, 0.75% (w/v) Iberian agar supplemented with 5% (v/v) horse serum and $MgCl_2$ to a final concentration of 25 mM) medium [15] and incubated for 72 h at 30 °C. A small sample of biomass was mixed with LPB (L-phase broth) medium [15] and images of vesicles were obtained using an Axio Lab A1 Microscope (Zeiss) equipped with an Axiocam 105 color camera (Zeiss) and ZEN 2.5 software (blue edition, Carl Zeiss Microscopy GmbH). The diameter of the five largest vesicles observed were measured in ImageJ [282] to confirm the presence of vesicles with a diameter larger than 2 µm. Isolates screening positive were subsequently incubated in LPB medium for 72 h at 30 °C and 100 rpm to determine vesicle formation in liquid culture (incubation up to 192 h was required for poor-growing strains). Nucleic acids were visualized with SYTO 9 at a final concentration of 2 µM and cell membranes with SynapseRed C2M at a final concentration of 40 $\mu g\,ml^{-1}$. For strains that only produced vesicles on LPMA medium, a sample of biomass was resuspended in LPB medium containing SYTO 9 and SynapseRed C2M. For fluorescence microscopy images the cell diameter was measured in ImageJ based on the SynapseRed C2M-stained membrane.

Supplementary Data

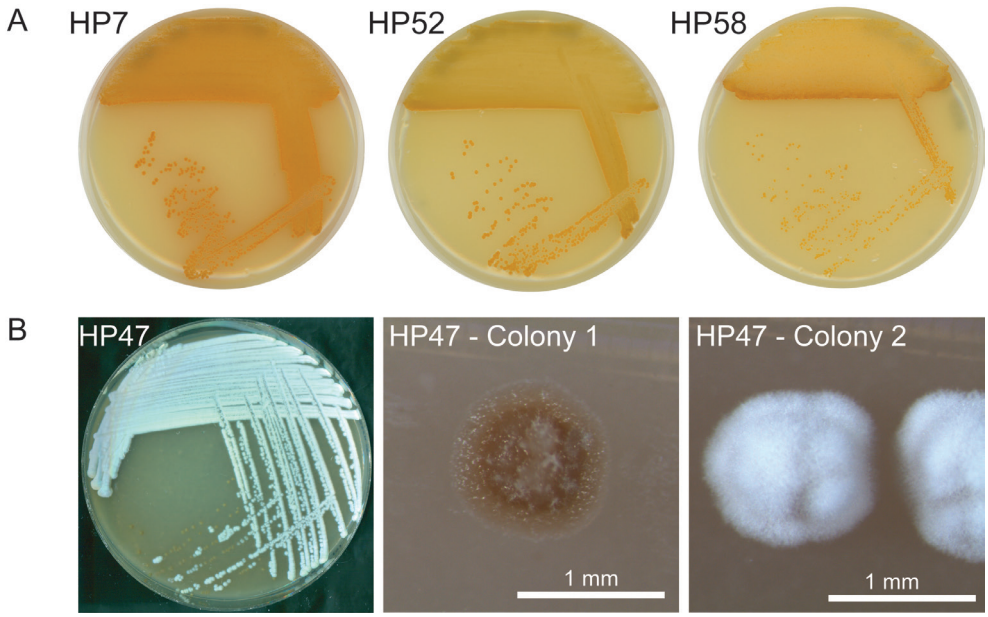

Supplementary Figure 1. Morphology of *Micromonospora* and *Pseudonocardia* isolates
(A) Morphology of *Micromonospora*-isolates HP7, HP52 and HP58 after 72 h growth on MS medium at 30 °C. **(B)** Morphology of *Pseudonocardia*-isolate HP47 grown for 72 h on MS medium at 30 °C. The right two stereomicroscopy images indicate the brown substrate mycelium (colony 1) and the formation of white aerial hyphae (colony 2).

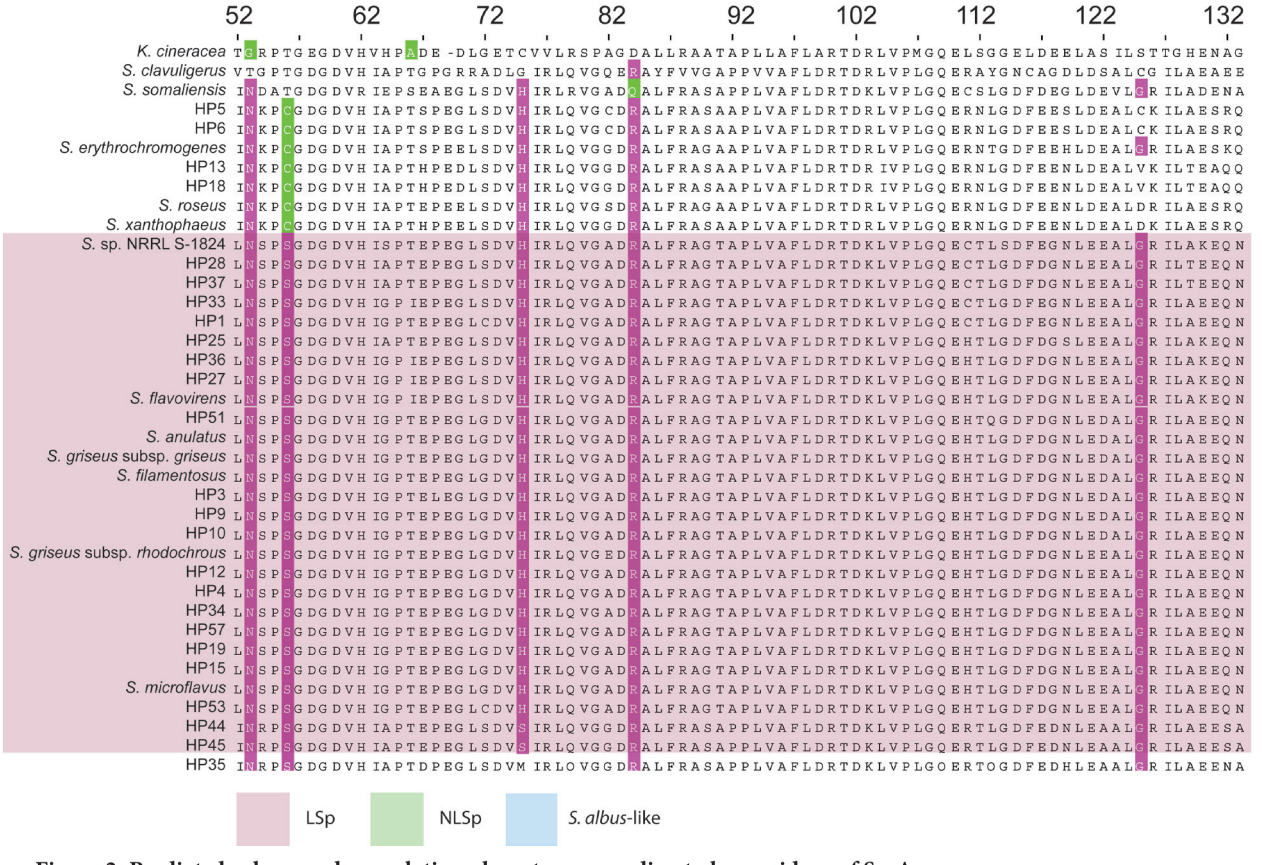

Supplementary Figure 2. Predicted submerged sporulation phenotype according to key residues of SsgA

Multiple sequence alignment of SsgA protein sequences (pos. 2 – 133 corresponding to *S. coelicolor* A3(2)) containing all strains present in Fig. 3. Only pos. 52 – 133 are shown. See Electronic Supplementary Data, Figure 1 for full alignment. Coloured residues indicate agreement with key residues typical of liquid-culture sporulation (LSp, magenta) or non-liquid-culture sporulation (NLSp, green) phenotypes [374]. Blue highlighting indicates residues typical of *S. albus*, which does not belong to either NLSp or LSp groups. Note that in case residues correspond to both *S. albus* SsgA protein sequence and SsgA in LSp/NLSp phenotypes, colouring is set according to the LSp/NLSp phenotypes. Background shading indicates the (predicted) submerged sporulation phenotype based on presence of all key amino acid residues in the SsgA protein sequence typical of LSp, NLSp or *S. albus*, as indicated.

Supplementary Figure 2. (Continued)

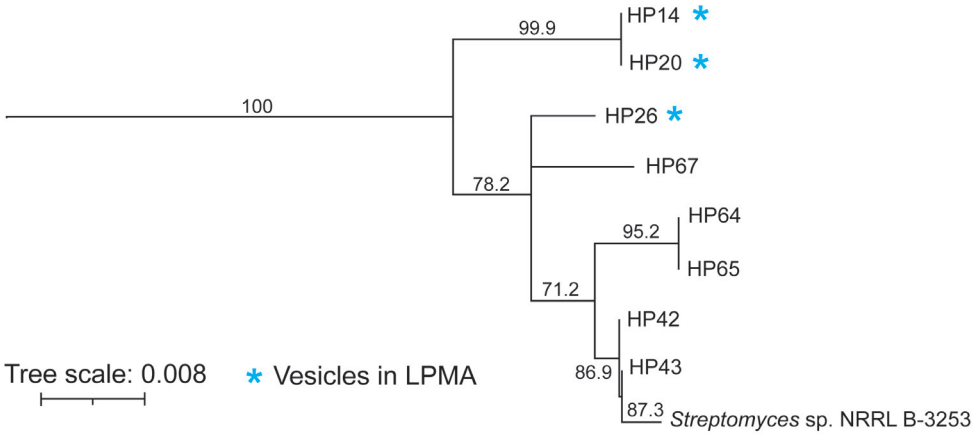

Supplementary Figure 3. Magnified section of *ssgA* nucleotide phylogenetic tree
Magnified section of the phylogenetic tree in Fig. 3 to clearly display the evolutionary relationships between isolates clustering with *Streptomyces* sp. NRRL B-3253. Asterisk (*) indicates the ability of HP isolates to produce vesicles on solid LPMA medium (blue).

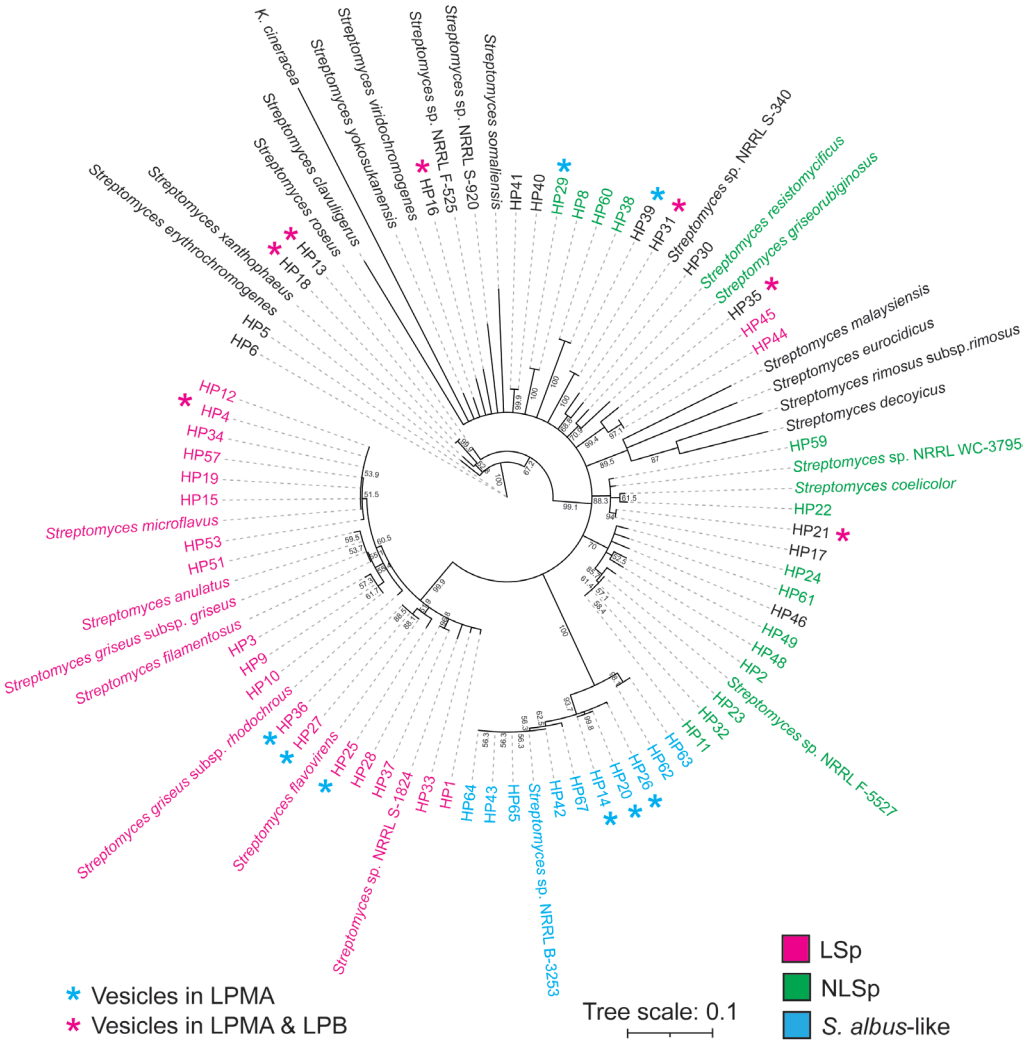

Supplementary Figure 4. Phylogenetic tree based on SsgA protein sequences

Neighbor-joining phylogenetic tree based on near-complete SsgA protein sequences (corresponding to *S. coelicolor* A3(2) SsgA amino acid position 3 – 133) of 58 wastewater isolates (HP) and 30 known *Streptomyces* strains and one *Kitasatospora* strain. The consensus tree was constructed based on the Neighbor-Joining algorithm with Tamura-Nei Genetic Distance model. The numbers at the nodes indicate bootstrap support values based on 1000 replicates. The scale bar represents 0.1 nucleotide substitution per position. Asterisks (*) indicate the ability to produce vesicles on solid LPMA and liquid LPB medium (magenta) or only on solid LPMA medium (blue), which was only tested for the HP isolates. Coloured text indicates the predicted submerged sporulation phenotype of the strain, namely liquid-culture sporulation (LSp, magenta), non-liquid-culture sporulation (NLSp, green) or a separate group with key residues corresponding to *S. albus*. Strains having only part of, or a mix of LSp or NLSp SsgA key residues are indicated with black text.

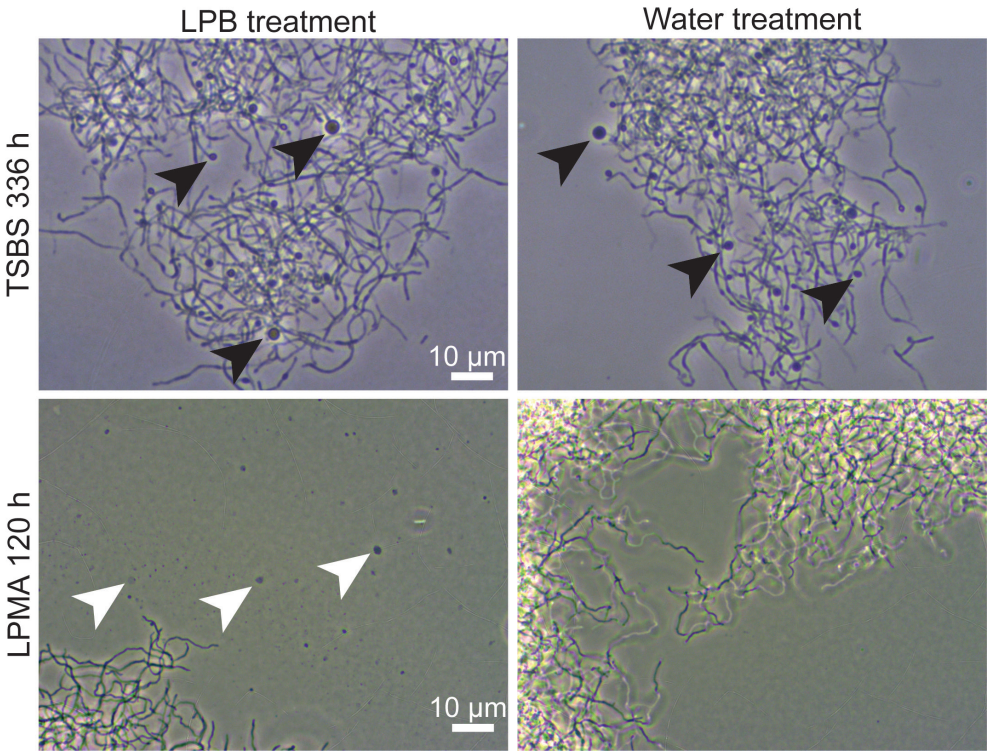

Supplementary Figure 5. Water sensitivity of spherical cells produced by isolate HP58
Isolate HP58 grown in liquid TSBS medium for 336 h, or grown on LPMA medium for 120 h, treated with LPB medium or water. Black arrows indicate putative spores, white arrows indicate vesicles. Note that water treatment only affected the vesicles observed under hyperosmotic stress conditions and not the spherical structures observed in TSBS medium.

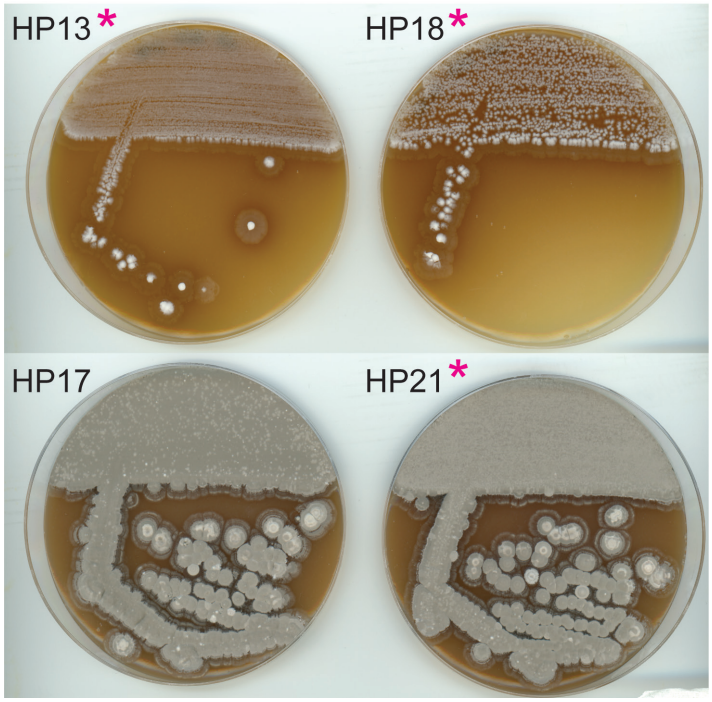

Supplementary Figure 6. Morphology of selected isolates on MS medium
Morphology of four isolates on MS medium incubated for 168 h at 30 °C and 168 h at room temperature. Isolate pairs HP13-HP18 and HP17-HP21 have similar morphologies and identical partial 16S rDNA and *ssgA* nucleotide sequences. Asterisk (magenta) indicates the ability to form vesicles on solid LPMA medium and in liquid LPB medium.

Supplementary Table 1. Overview of wastewater isolates.
The sample type from which strains were isolated (column S) are indicated as 1: before primary sedimentation, 2: activated sludge, 3: Nonidet-treated activated sludge, 4: after primary sedimentation. Medium used for initial isolation (column M) is indicated as MS: Mannitol Soya Flour medium, MM: Minimal medium, SC: Starch Casein medium, CD: Czapek-Dox agar, HV: Humic acid Vitamin agar. Top hit(s) to the database of EzBioCloud [364] are based on partial 16S rDNA sequences. In case of multiple top hits with identical pairwise similarity (P.S. %), all top hits are shown. The length of the nucleotide sequence used as a query is given (column Nt.) as well as the number of mismatches with the top hit (column M.M.).

Isolate	S	M	Top hit(s)	Strain	P.S. (%)	M.M.	Nt.
HP1	1	MS	*Streptomyces laculatispora*	BK166	99.64	5	1383
HP2	1	MM	*Streptomyces pseudogriseolus*	NRRL B-3288	100.00	0	1168
			Streptomyces werraensis	NBRC 13404	100.00	0	1168
			Streptomyces gancidicus	NBRC 15412	100.00	0	1167
HP3	1	MM	*Streptomyces pluricolorescens*	NBRC 12808	99.44	6	1081
			Streptomyces rubiginosohelvolus	NBRC 12912	99.44	6	1081
HP4	1	SC	*Streptomyces cavourensis*	NBRC 13026	99.92	1	1196
HP5	1	SC	*Streptomyces subrutilus*	DSM 40445	99.10	10	1105
HP6	1	SC	*Streptomyces sporoverrucosus*	NBRC 15458	99.59	5	1226
			Streptomyces goshikiensis	NBRC 12868	99.59	5	1226
HP7	1	SC	*Micromonospora aurantiaca*	ATCC 27029	99.83	2	1194
HP8	2	CD	*Streptomyces humidus*	NBRC 12877	99.49	6	1188
HP9	2	CD	*Streptomyces badius*	NRRL B-2567	99.49	6	1169
			Streptomyces parvus	NBRC 3388	99.49	6	1169
			Streptomyces pluricolorescens	NBRC 12808	99.49	6	1169
			Streptomyces rubiginosohelvolus	NBRC 12912	99.49	6	1169
HP10	2	CD	*Streptomyces badius*	NRRL B-2567	99.40	7	1162
			Streptomyces parvus	NBRC 3388	99.40	7	1162
			Streptomyces pluricolorescens	NBRC 12808	99.40	7	1162
			Streptomyces rubiginosohelvolus	NBRC 12912	99.40	7	1162
HP11	2	CD	*Streptomyces griseoincarnatus*	LMG 19316	99.65	4	1159
			Streptomyces labedae	NBRC 15864	99.65	4	1159
HP12	2	CD	*Streptomyces setonii*	NRRL ISP-5322	100.00	0	1141
			Streptomyces anulatus	NRRL B-2000	100.00	0	1141
			Kitasatospora papulosa	NRRL B-16504	100.00	0	1141
			Streptomyces pratensis	ch24	100.00	0	1141
HP13	2	MS	*Streptomyces xanthophaeus*	NRRL B-5414	100.00	0	1151
			Streptomyces nojiriensis	LMG 20094	100.00	0	1151
			Streptomyces spororaveus	LMG 20313	100.00	0	1151

Supplementary Table 1. (Continued)

Isolate	S	M	Top hit(s)	Strain	P.S. (%)	M.M.	Nt.
HP14	2	MS	*Streptomyces albidoflavus*	DSM 40455	99.26	8	1084
HP15	2	MS	*Streptomyces microflavus*	NBRC 13062	100.00	0	1334
			Streptomyces fulvorobeus	NBRC 15897	100.00	0	1333
HP16	2	MS	*Streptomyces recifensis*	NBRC 12813	98.89	13	1174
HP17	2	MS	*Streptomyces caelestis*	NRRL 2418	98.25	20	1142
HP18	2	MS	*Streptomyces xanthophaeus*	NRRL B-5414	99.83	2	1198
			Streptomyces nojiriensis	LMG 20094	99.83	2	1198
			Streptomyces spororaveus	LMG 20313	99.83	2	1198
HP19	2	MS	*Streptomyces microflavus*	NBRC 13062	99.35	8	1235
HP20	2	MS	*Streptomyces albidoflavus*	DSM 40455	98.98	12	1173
HP21	2	MS	*Streptomyces caelestis*	NRRL 2418	99.18	11	1342
HP22	2	MS	*Streptomyces coelicoflavus*	NBRC 15399	100.00	0	1151
HP23	2	HV	*Streptomyces thermocarboxydus*	DSM 44293	99.59	5	1217
HP24	2	HV	*Streptomyces thermocarboxydovorans*	DSM 44296	98.40	18	1126
HP25	2	HV	*Streptomyces halstedii*	NBRC 12783	99.83	2	1197
HP26	2	MM	*Streptomyces albidoflavus*	DSM 40455	99.58	5	1194
HP27	2	MM	*Streptomyces setonii*	NRRL ISP-5322	99.76	3	1228
			Streptomyces anulatus	NRRL B-2000	99.76	3	1228
			Kitasatospora papulosa	NRRL B-16504	99.76	3	1228
			Streptomyces pratensis	ch24	99.76	3	1228
HP28	2	MM	*Streptomyces drozdowiczii*	NBRC 101007	98.98	13	1278
HP29	2	MM	*Streptomyces humidus*	NBRC 12877	99.51	5	1026
HP30	2	MM	*Streptomyces fumigatiscleroticus*	NBRC 12999	98.94	12	1136
HP31	2	SC	*Streptomyces indiaensis*	NBRC 13964	98.66	15	1120
HP32	2	SC	*Streptomyces albogriseolus*	NRRL B-1305	99.23	8	1042
HP33	2	SC	*Streptomyces brevispora*	BK160	99.35	8	1237
HP34	2	SC	*Streptomyces cavourensis*	NBRC 13026	100.00	0	1307
HP35	2	SC	*Streptomyces laurentii*	ATCC 31255	98.37	18	1105
HP36	3	CD	*Streptomyces griseus* subsp. *griseus*	KCTC 9080	98.77	14	1134
HP37	3	MS	*Streptomyces drozdowiczii*	NBRC 101007	99.15	10	1174
HP38	3	MS	*Streptomyces rhizosphaerihabitans*	JR-35	97.60	28	1169
HP39	3	MS	*Streptomyces indiaensis*	NBRC 13964	98.69	15	1143
HP40	3	MS	*Streptomyces achromogenes* subsp. *achromogenes*	NBRC 12735	99.48	6	1149

Supplementary Table 1. (Continued)

Isolate	S	M	Top hit(s)	Strain	P.S. (%)	M.M.	Nt.
HP41	3	MS	*Streptomyces achromogenes* subsp. *achromogenes*	NBRC 12735	99.91	1	1068
HP42	3	MS	*Streptomyces albidoflavus*	DSM 40455	99.54	5	1078
HP43	3	MS	*Streptomyces daghestanicus*	NRRL B-5418	99.66	4	1177
			Streptomyces albidoflavus	DSM 40455	99.66	4	1177
HP44	3	HV	*Streptomyces zaomyceticus*	NBRC 13348	99.66	4	1184
HP45	3	HV	*Streptomyces zaomyceticus*	NBRC 13348	99.75	3	1201
HP46	3	HV	*Streptomyces althioticus*	NRRL B-3981	99.66	4	1176
HP47	3	HV	*Pseudonocardia carboxydivorans*	Y8	99.91	1	1167
HP48	3	HV	*Streptomyces marokkonensis*	Ap1	99.16	10	1197
			Streptomyces lienomycini	LMG 20091	99.16	10	1197
HP49	3	MM	*Streptomyces marokkonensis*	Ap1	98.33	19	1135
HP51	3	MM	*Streptomyces setonii*	NRRL ISP-5322	99.28	8	1113
			Streptomyces anulatus	NRRL B-2000	99.28	8	1113
			Kitasatospora papulosa	NRRL B-16504	99.28	8	1113
			Streptomyces pratensis	ch24	99.28	8	1113
HP52	3	MM	*Micromonospora fluminis*	A38	99.63	4	1086
HP53	3	SC	*Streptomyces setonii*	NRRL ISP-5322	99.76	3	1230
			Streptomyces anulatus	NRRL B-2000	99.76	3	1230
			Kitasatospora papulosa	NRRL B-16504	99.76	3	1230
			Streptomyces pratensis	ch24	99.76	3	1230
HP57	3	SC	*Streptomyces cavourensis*	NBRC 13026	99.66	4	1173
HP58	3	SC	*Micromonospora vinacea*	GUI63	99.22	9	1160
HP59	4	CD	*Streptomyces marokkonensis*	Ap1	98.78	14	1144
HP60	4	MS	*Streptomyces variegatus*	NRRL B-16380	98.05	23	1179
HP61	4	HV	*Streptomyces prasinus*	NRRL B-2712	99.58	5	1180
HP62	4	MM	*Streptomyces diastaticus*	NBRC 3714	97.92	23	1107
HP63	4	MM	*Streptomyces diastaticus*	NBRC 3714	100.00	0	1355
HP64	4	SC	*Streptomyces albidoflavus*	DSM 40455	99.52	5	1044
HP65	4	SC	*Streptomyces albidoflavus*	DSM 40455	100.00	0	1379
HP67	4	SC	*Streptomyces intermedius*	NBRC 13049	99.13	10	1144

Supplementary Table 2. Overview of closely related HP isolates.
HP isolates having either identical partial 16S rDNA or *ssgA* sequences are shown. Pairs are sorted based on percent 16S rDNA sequence identity followed by percent *ssgA* nucleotide (nt) identity. The percent identity between the amino acid sequence of SsgA is given (SsgA protein % identity), with the number of differing amino acids indicated between brackets. In addition, the ability to produce vesicles is indicated by underscoring (vesicles only observed on solid LPMA medium) or with an asterisk (*) (vesicles observed upon growth on LPMA medium and in liquid LPB medium).

Isolate 1	Isolate 2	16S rDNA % identity	*ssgA* nt % identity	SsgA protein % identity
HP44	HP45	100	100	100
HP28	HP37	100	100	100
HP13*	HP18*	100	100	100
HP17	HP21*	100	100	100
HP31*	HP39	100	100	100
HP14	HP20	100	100	100
HP42	HP43	100	100	100
HP38	HP60	100	99.75	100
HP42	HP65	100	99.24	100
HP42	*S.* sp. NRRL B-3253	100	99.75	100
HP43	HP65	100	99.24	100
HP43	*S.* sp. NRRL B-3253	100	99.75	100
HP65	*S.* sp. NRRL B-3253	100	98.98	100
HP15	*S. microflavus*	100	98.98	100
HP2	*S.* sp. NRRL F-5527	100	95.69	98.47 (2 aa)
HP25	HP27	100	91.12	97.71 (3 aa)
S. flavovirens	*S. anulatus*	100	85.53	96.18 (5 aa)
HP8	HP29	99.92	100	100
HP5	HP6	99.78	100	100
HP40	HP41	99.75	100	100
HP64	HP65	99.22	100	100
HP9	HP10	99.11	100	100
HP15	HP19	99.00	100	100
HP4*	HP34	98.83	100	100
HP62	HP63	98.11	100	100

Supplementary Table 3. Vesicle diameters

Diameters (µm) of largest imaged vesicles released by wastewater isolates after 72 h growth on LPMA medium. Cells were resuspended in LPB medium and imaged using the Zeiss Axioscope A.1. Measurements were based on the five largest vesicles captured by imaging to confirm the presence of vesicles with a diameter larger than 2 µm to differentiate them from spores.

Isolate	D_{min}	D_{max}	D_{avr}	D_{stdev}
HP4	1.77	3.11	2.27	0.64
HP13	1.13	2.08	1.69	0.44
HP14	1.54	2.96	2.24	0.63
HP16	1.29	2.12	1.77	0.33
HP18	1.68	2.37	1.97	0.31
HP20	1.81	2.43	2.02	0.26
HP21	1.04	3.08	2.06	0.90
HP25	1.60	2.31	1.88	0.26
HP26	1.22	2.85	1.89	0.67
HP27	1.08	2.21	1.75	0.55
HP29	1.33	2.75	2.06	0.56
HP31	1.54	2.82	2.03	0.54
HP35	1.29	2.62	2.01	0.48
HP36	1.56	2.04	1.84	0.19
HP39	1.36	3.19	2.28	0.80
HP58	2.19	2.83	2.52	0.25

Supplementary Table 4. Overview of isolation media.
Isolation media used for the first round of selective isolation of filamentous actinobacteria from wastewater. All media were supplemented with a final concentration of 50 µg mL^{-1} nystatin and 10 µg mL^{-1} nalidixic acid.

Medium	Components (per L prepared medium)	Carbon source (primary)	Reference
Humic acid Vitamin agar (HV)	1 g Humic acid (Sodium Salt, Acros Organics, 50-60% as humic acid); 0.5 g Na_2HPO_4 (Sigma); 1.71 g KCl (Sigma); 0.05 g $MgSO_4 \times 7\ H_2O$ (Sigma); 0.01 g $FeSO_4 \times 7\ H_2O$ (Merck); 0.02 g $CaCO_3$ (Janssen Chimica), B-vitamins mixture*; 18 g agar	Humic Acid	407
Czapek-Dox agar (CD)	30 g sucrose, 3 g $NaNO_3$, 1 g K_2HPO_4, 0.5 $MgSO_4$, 0.5 KCl, 0.01 $FeSO_4$, 20 g agar	Sucrose	BD Difco™ Czapek-Dox Broth
Starch Casein agar (SC)	10 g soluble starch (Baker Analyzer), 0.3 g vitamin-free casein (Sigma), 2 g KNO_3 (Sigma), 2 g NaCl (Sigma), 3.35 g $K_2HPO_4 \times 3H_2O$ (Sigma)), 0.05 g $MgSO_4 \times 7H_2O$ (Sigma)), 0.02 g $CaCO_3$ (Janssen Chimica), 0.02 g $FeSO_4 \times 7H_2O$ (Merck), 20 g agar.	Starch	408
Mannitol soya flour medium (MS)	20 g soya flour, 20 g mannitol, 20 g agar	Mannitol	326
Minimal Medium (MM)	1% glycerol, 20 g agar	Glycerol	223

* B-vitamin mixture contains: thiamine hydrochloride, riboflavin, niacin, pyridoxine hydrochloride, inositol, calcium pantothenate, 4-aminobenzoic acid (0.5 mg L^{-1} each) and 0.25 mg mg L^{-1} biotin.

Supplementary Table 5. Overview of extracted *ssgA* nucleotide sequences
The *ssgA* nucleotide sequences were extracted with 500 bp flanks from StrepDB and used to design degenerate primers for *ssgA* amplification.

Scientific name	StrepDB gene identifier	Reference
Streptomyces clavuligerus	SCLAV_2865	374
Streptomyces griseus subsp. *griseus* NBRC 11350	SGR_3655	374
Streptomyces venezuelae ATCC 10712	SVEN_3705	374
Streptomyces sp. S4	STRS4_05858	374
Streptomyces avermitilis NBRC 14893	SAV_4267	374
Streptomyces scabies	SCAB46311	374
Streptomyces coelicolor A3(2)	SCO3926	374
Streptomyces lividans 1326	SLI_4184	StrepDB
Streptomyces leeuwenhoekii	sle_36430	StrepDB

Supplementary Table 6. Overview of representative *Streptomyces* and *Kitasatospora* stains used.
The locus_tag is provided for the extracted 16S rDNA and *ssgA* nucleotide sequences.

Scientific name	16S rDNA	*ssgA*
Streptomyces xanthophaeus NRRL B-5414	IO30_RS41010	IO30_RS0109850
Streptomyces roseus ATCC 31245	ACS04_00550	ACS04_09320
Streptomyces erythrochromogenes NRRL B-2112	IO28_RS35905	IO28_RS0128825
Streptomyces somaliensis DSM 40738	M4914_RS03860	M4914_RS18135
Streptomyces sp. NRRL B-3253	IO21_RS0127920	IO21_RS0114100
Streptomyces sp. NRRL F-525	OO69_RS48035	OO69_RS39545
Streptomyces resistomycificus DSM 40133	AQJ84_RS40195	AQJ84_RS17070
Streptomyces griseorubiginosus DSM 40469	AQJ54_RS42895	AQJ54_RS32550
Streptomyces viridochromogenes NRRL 3416	ADK35_RS10715	ADK35_RS04220
Streptomyces yokosukanensis DSM 40224	AQI95_RS44000	AQI95_RS00825
Streptomyces sp. NRRL S-340	IG64_RS37070	IG64_RS15575
Streptomyces sp. NRRL F-5527	IH17_RS0135660	IH17_RS0105615
Streptomyces sp. NRRL WC-3795	IH30_RS0134315	IH30_RS0114480
Streptomyces sp. NRRL S-1824	IG01_RS42290	IG01_RS0116010
Streptomyces flavovirens NRRL B-2182	IG72_RS35440	IG72_RS0100835
Streptomyces microflavus DSM 40593	HUT09_RS26785	HUT09_RS17350
Streptomyces griseus subsp. *rhodochrous* NRRL B-2932	IF87_RS0134015	IF87_RS0101640
Streptomyces anulatus ATCC 11523	JI76_RS28310	JI76_RS17700
Streptomyces filamentosus NRRL 11379	SSIG_RS18710	SSIG_RS16150
Streptomyces eurocidicus ATCC 27428	AF335_RS10775	AF335_RS12920
Streptomyces decoyicus NRRL 2666	K7C20_RS27780	K7C20_RS19325
Streptomyces rimosus subsp. *rimosus* NRRL WC-3558	IH19_RS0142600	IH19_RS0107250
Kitasatospora cineracea DSM 44780	Consensus of EDD39_RS11390; EDD39_RS18015; EDD39_RS17275; EDD39_RS33940; EDD39_RS33370; EDD39_RS32005; EDD39_RS12480; EDD39_RS04560; EDD39_RS00010	EDD39_RS06390
Streptomyces malaysiensis DSM 4137	Consensus of DNK48_RS40295; DNK48_RS34750; DNK48_RS27680; DNK48_RS22170; DNK48_RS21675; DNK48_RS14635	DNK48_RS23965
Streptomyces sp. NRRL S-920	IG54_RS38845	IG54_RS0109940
Streptomyces coelicolor A3(2)	SCOr06 (*rrnB*)	SCO3926
Streptomyces griseus subsp. *griseus* NBRC 13350	SGR_RS30675	SGR_RS18100
Streptomyces clavuligerus ATCC 27064	SCN_RS39020	SCN_RS13850

Electronic Supplementary Data

Electronic Supplementary Figure 1 is available on the online repository OSF database and can be accessed via: https://doi.org/10.17605/OSF.IO/M6XUW

Electronic Supplementary Figure 1. Predicted submerged sporulation phenotype according to key residues of SsgA

Full multiple sequence alignment of SsgA protein sequences (pos. 2 – 133 corresponding to *S. coelicolor* A3(2)) containing all strains present in Fig. 3. Coloured residues indicate agreement with key residues typical of liquid-culture sporulation (LSp, magenta) or non-liquid-culture sporulation (NLSp, green) phenotypes. Blue highlighting indicates residues typical of *S. albus*, which does not belong to either NLSp or LSp groups. Note that in case residues correspond to both *S. albus* SsgA protein sequence and SsgA in LSp/NLSp phenotypes, colouring is set according to the LSp/NLSp phenotypes. Background shading indicates the (predicted) submerged sporulation phenotype based on presence of all key amino acid residues in the SsgA protein sequence typical of LSp, NLSp or *S. albus*, as indicated.